2006 中華民國航太學會/中華民航學會聯合學術研討會

投稿範圍： 【請務必圈選】

□ 1. 氣動力學	□ 2. 實驗與計算流體力學	□ 3. 燃燒與熱質傳
□ 4. 噴射推進與渦輪引擎	□ 5. 航太結構及先進材料	□ 6. 飛行力學
□ 7. 航太電子及通訊	□ 8. 控制與導引	□ 9. 全球定位系統
□ 10. 天體力學	□ 11. 旋翼機	□ 12. 微系統科技
□ 13. 航太實驗設備與測試	□ 14. 航太系統與次系統	□ 15. 航太製造及維修
□ 16. 適航認證	□ 17. 民航法規與制度	□ 18. 航太品保
□ 19. 飛航及安全管理	□ 20. 航空資訊技術	□ 21. 航空經濟與財務
□ 22. 民航飛行技術	□ 23. 空域規劃與管理	□ 24. 航太醫學
□ 25. 微微衛星系統工程＊	□ 26. 航太科技教育＊	□ 27. 其他航太相關應用

題目： Accuracy Comparison between Two Sharp and Diffusive Filters

作者（中文）： 鄭育能 鄭又齊

作者（英文）： Yih-Nen Jeng & You-Chi Cheng

若投稿論文為國科會研究計畫之成果，請註明國科會計畫編號：
NSC 94-2212-E-006-084

欲參加『青年會員論文』獎或『學生論文競賽』獎競賽者請勾選（至多勾選一項，參賽資格請見徵文啟事）：

□ 『青年會員論文』獎
□ 『學生論文競賽』獎

聯絡人： 鄭育能
單位： 國立成功大學航空太空工程學系；
地址： 台南市大學路一號
電話： 06-2757575 ext.63685
傳真： 06-2389940
E-mail： z6208016@email.ncku.edu.tw

Accuracy Comparison between Two Sharp and Diffusive Filters

Yih-Nen Jeng[1], You-Chi Cheng[2]
[1] Department of Aeronautics & Astronautics, National Central university
[2] Department of Electrical Engineering, National Taiwan university
NSC Project No.：NSC-94-2212-E-006-084

Abstract

The error comparison of the resulting smooth parts generated by two sharp high/low passed filters is performed numerically. The first filter employs the linear trend removal and a Fast Fourier Transform (FFT) algorithm and the second filter employs the iterative and diffusive filter and the FFT algorithm. After removing the non-sinusoidal and low frequency parts, both methods generate the spectrum of the high frequency part. The subsequent filtering step is finished by impose rectangular window to the spectrum. A given test case shows that the second filter is convenient and can achieve the error level specified by the iterative filter and data resolution. If the desired high frequency part of the data string has a zero value at the two data ends, the resulting error of the first filter is much better than that of the second filter. For a general case, the error level of the smooth part generated by the second filter is smaller than that of the first filter. The test of a turbulent flow data string shows the procedure of employing the sharp filter with iterative Gaussian smoothing.

Keywords：sharp filters, error comparison.

1. Introduction

Because of the rapid development of computer hardware and software, the capability of collecting huge number of long data string increases rapidly. Generally, a real data string frequently has a complex structure which changes main characters rapidly. People might hope that the Fourier spectrum can be considered as a parameter representation of time series data, $y_0, y_1, ..., y_n$, where n is the data size [1-2]. Unfortunately, the Fourier spectrum is an exact parameter representation of the original data only if the data and all the derivatives up to $(n-1)$ th order are periodic. Since most data string can not satisfy these restrictions simultaneously, the corresponding discrete Fourier spectrum at most represents the original data string in a weak sense. In other words, a Fourier spectrum frequently involve certain minor errors such that some dominant modes are slightly distorted and almost all minor modes are seriously faded. In Ref.[3-10], an approximate Fourier sine spectrum was proposed to replace the Fourier spectrum. Note that a Fourier sine spectrum requires $y = 0$ at two ends and odd function properties. In order to satisfy these requirements, finite segments around the two ends should be discarded and the non-sinusoidal part must be removed. Therefore, most of the resulting Fourier sine spectrums may slightly deviate form their corresponding Fourier spectrums.

In Ref.[4-10], The non-sinusoidal part is estimated by the smooth part generated by the iterative and diffusive filter. Unfortunately, the transition zone of the filter cannot be made sharp enough with a reasonable computing time. In Ref.[11], two simple and fast sharp filters are proposed: one employs the linear trend removal and an FFT algorithm and the second filter employs the iterative and diffusive filter and the FFT algorithm. However, their precise performances are not compared. This study examines their errors.

2. Theoretical Development

2.1 The Sharp Filter Using the Iterative Gaussian Smoothing

2.1.1 The Iterative Gausian Smoothing

Consider a set of data $(t_i, y_i), i = 0, N$. After employing the Gaussian smoothing method [3-10], the smooth response is

$$\bar{y}_{1,j} = \frac{1}{L}\sum_{i=0}^{N} y_i e^{-(t_i - t_j)^2/2\sigma^2},\ L = \sum_{i=0}^{N} e^{-(t_i - t_j)^2/2\sigma^2} \quad (1)$$

The iterative Gaussian smoothing employs the following procedure:

1. Given the smoothing factor σ and iteration step m;
2. Employ the Gaussian smoothing to smooth the data and obtain $\bar{y}_{1,j}$ and $y'_{1,j}$, where $\bar{y}_{1,j}$ is the smoothed part, and $y'_{1,j}$ is the high frequency part.
3. Repeatedly smooth the high frequency part, $y'_{k,j}$, $k = 1,2,..., m$.
4. $y'_{m,j}$ is the desired high frequency part and $y_j - y'_{m,j}$ is the smooth part.

If the original data is expressed in the following form

$$y(t_i) = \sum_{n=0}^{N} b_n \cos\left(\frac{2\pi t_i}{\lambda_n}\right) + c_n \sin\left(\frac{2\pi t_i}{\lambda_n}\right) \quad (2)$$

The first smooth part is

$$\bar{y}_{1,i} \approx \sum_{n=0}^{N} a(\sigma/\lambda_n)\{b_n \cos\left(\frac{2\pi t_i}{\lambda_n}\right) + c_n \sin\left(\frac{2\pi t_i}{\lambda_n}\right)\}$$

$$a(\sigma, \lambda_l) = \frac{1}{L}\sum_{i=0}^{N} e^{-t_i^2/(2\sigma^2)} \cos\frac{2\pi t_i}{\lambda_l} \quad (3)$$

For the interior points remote from 0 and N, it can be proven that

$$a(\sigma/\lambda_n) \approx \exp[-2\pi^2\sigma^2/\lambda_n^2] \le 1 \quad (4)$$

It can also been proven that

$$\bar{y}_i = \bar{y}_{1,i} + \bar{y}_{2,i} + ... + \bar{y}_{m,i} = y_i - y'_{m,i}$$
$$= \sum_{n=0}^{N} A_{n,m,\sigma}\left[b_n \cos\left(\frac{2\pi t_i}{\lambda_n}\right) + c_n \sin\left(\frac{2\pi t_i}{\lambda_n}\right)\right] \quad (5)$$

Similarly, the interior points remote from 0 and N

$$A_{n,m,\sigma} \approx 1-[1-\exp\{-4\pi^2\sigma^2/\lambda_n^2)]^m$$
$$0 \le A_{n,m,\sigma} \le 1 \quad (6)$$

such that the iterative filter is diffusive. The smoothing factor σ and iteration steps m are solved from a given transition zone $(\lambda_c, \bar{\lambda})$

$$1-[1-\exp(-4\pi^2\sigma^2/\lambda_c^2)]^m = \delta$$
$$1-[1-\exp(-4\pi^2\sigma^2/\bar{\lambda}^2)]^m = 1-\delta \quad (7)$$

where δ is an user specified parameter.

2.2 The Fourier Sine Spectrum Generator

A careful examination upon the discrete Fourier transform [1,2] reveals that, for a perfect Fourier expansion, the necessary periodic conditions should be held for all y, y', …, and $y^{(N-1)}$. Unfortunately, most data can not satisfy such severe restrictions. If the data involves the non-sinusoidal part, the resulting spectrum will be contaminated by the resulting Fourier components which run over the whole spectrum domain and is often referred as the Direct Current (DC) contamination. Consequently, current spectrums of most data strings are projections in weak sense. According to numerical experiments, the weak projection leads to two undesired imperfections: minor modes are seriously faded and dominated modes are slight distorted.

In ref.[3-10], the iterative Gaussian smoothing is employed to remove the non-sinusoidal part. Since the iterative Gaussian smoothing has error around the two ends, data segments around the two ends of the remaining sinusoidal part should be dropped. A search procedure and an interpolation method are employed to locate zero values of sinusoidal part. The data string beyond these zero points should be further dropped. After employing the modified monotonic cubic interpolation [1,12] to redistribute the sinusoidal data so as to obtain data size to be integer power of 2, the odd function mapping makes sure that all the periodic conditions are satisfied. Since the cubic interpolation procedure is employed and data segments are dropped around the two ends, the resulting Fourier sine spectrum will slightly deviate from the original sinusoidal part's spectrum. It is believed that the spectrum error is approximately equal to the smallest possible level.

2.3 Two Sharp and Diffusive Filters

2.3.1 The First Sharp filter [11]

2.3.1.1 The Linear Trend Removal

A convenient method to remove the non-sinusoidal part is to assume the sinusoidal part taking zero values at the two data ends. The non-sinusoidal part is just the linear interpolation between the two end points and the sinusoidal part is the result by subtracting the linear interpolation from the original data. In general, this approach does not work. However, it provides a simple method to remove a large fraction of the non-sinusoidal part. Therefore, the linear trend removal is employed to first estimate the non-sinusoidal part. Since the zero value points around the two ends of a data string is generally not just the two ends, it is recommended to estimate the possible zero value points.

2.3.1.2 The Sharp Filter Using the Linear Trend Removal and Fourier Sine Spectrum Generator

The first sharp filter employs the linear trend removal and Fourier sine spectrum generator. Its procedure is listed below.

1. Properly choose two end points of the data string. Drop data segments beyond the two points.
2. Use the linear trend removal so that the data string has zero value at the two ends.
3. Use the Fourier sine spectrum generator to find the spectrum.
4. Choose the desired cut-off frequency and perform the inverse Fourier transform of the modes whose frequency is smaller than the cut-of frequency. Add this inversed data to the linear part removed by the linear trend removal. The resulting data is the smoothed part.
5. Find the Fourier sine spectrum of the remaining high frequency part. Again, remove the modes whose frequencies are small than the cut-off frequency.
6. The other sharp band-passed limited spectrum can be directly obtained by embedding unit rectangular window on the spectrum. The band-passed limited data string is the corresponding inverse Fourier transform.

2.3.2 The Second Sharp Filter

The required number of the iteration steps, m becomes an incredibly large number for a narrow transition zone. Note that, if the Fourier spectrum is exact, the step function type filter imposing on the spectrum gives a diffusive filtering response too. If the data length is long enough to make sure that $\bar{\lambda} < 0.1t_N$, the iterative filter can employ a relative wide transition zone, for example, $\bar{\lambda}/\lambda_c = 3$, Eqs.(7) gives $m \approx 17$ and $\sigma/\lambda_c = 0.701712$. After cutting data segments around the two ends whose lengths $\approx 6\sigma$, the Fourier

sine spectrum generator of previous sub-section gives a spectrum with small error. Finally, the sharp and diffusive filtering procedure with cutting frequency at λ_c gives the high-passed spectrum by eliminating all modes of the spectrum whose $\lambda > \lambda_c$. For the sake of demonstrating the resulting error, the corresponding results will not cut segments around the two ends.

The second sharp filter basing on the iterative Gaussian smoothing is composed of the following procedure:

1. Use an FFT algorithm to estimate the Fourier spectrum of a data string.
2. Determine the cut-off frequency corresponding to λ_c and $\bar{\lambda}$.
3. Find the corresponding smooth factor σ and iteration step m by solving Eqs.(7).
4. Perform the iterative filter basing on the iterative Gaussian smoothing to obtain the estimated smoothed and high frequency part.
5. Find the Fourier sine spectrum of the estimated high frequency part.
6. Remove all the modes whose $\lambda > \lambda_c$ and find the resulting high frequency part. The difference between the original data and this high frequency part is the smooth part.
7. The other sharp band-passed limited spectrum can be directly obtained by embedding unit block window on the spectrum. The band-passed limited data string is the corresponding inverse Fourier transform.

2.4 A New Spectrogram Generator [7,8]

A previous study showed that both the Morlet and Gabor transforms impose a Gaussian window on time domain and cause a corresponding Gaussian window on the spectrum. Since the Fourier sine spectrum generator gives an accurate spectrum. it was proposed to direct impose a window on the spectrum domain. If a Gaussian window is employed, the corresponding inverse FFT will give

$$y_k(\tau) = \sum_{n=0}^{N-1}(b_n - jc_n)e^{j2\pi\tau/\lambda_n}e^{-(n-k)^2/(2c^2)} \qquad (8)$$

where the center frequency of the window is located at $f_k = k/t_N$. After scanning all the desired frequency, the corresponding spectrogram can be obtained.

3. Results and Discussions

The following composite wave is employed to examine the error of the smooth part generated by two sharp filters, respectively.

$$\begin{aligned} y_i &= 1 + 0.2t_i + 0.025{t_i}^2 + 1.3e^{-0.05{t_i}^2}\sin(0.6\pi t_i) \\ &\quad + 0.8\sin(10\pi t_i) + 0.7\sin(5.6\pi t_i) \\ &\quad + 0.3(1 + 0.2t_i + 0.01{t_i}^2)e^{-0.005{t_i}^2}\sin(3.2\pi t_i) \\ x_i &= i\Delta x + d \end{aligned} \qquad (9)$$

where the first line of the equation represents the non-sinusoidal and low frequency parts and the second and third lines are the high frequency part. The parameter $d = 0$ for the case of sinusoidal part takes a zero value at the two ends, and $d = \pi/4$ for non-zero end case.

Figure 1 is the result of the first sharp filter with $d = 0$ in Eq.(9) where the cut-off frequency is set at $f = 1$ Hz. The figure shows that the simple method works very well, the largest error is approximately equal to 10^{-3}. By taking $\lambda_c = 0.625$ (i.e. $f = 1.6$ Hz) and $\bar{\lambda}/\lambda_c = 4$, the smooth result of employing the second sharp filter has the error distribution shown in Fig.2. By decreasing the error level of iteration to be $\delta = 0.0001$, the error distribution in the interior regions where $3 < t < 7$ is approximately equal the that shown in Fig.1. However, around the two ends, the error of Fig.2 is obviously larger than that shown in Fig.1 because of the error introduced by the iterative Gaussian smoothing. As a first conclusion for the case where the high frequency part takes a zero value at the two ends, it seems that the performance of the first sharp filter is better than that of the second sharp filter.

For the test case with $d = \pi/4$, where the high frequency part is not zero, the result of the first sharp filter without dropping data around the two ends is shown in Fig.3. The resulting error distribution is much worse than that shown in Fig.1. The reason is that the estimation of the linear trend removal is not good around the two ends. As a consequence, the estimated smooth part is seriously deviated from the original smoothed part. Figure 4 shows the error response of dropping segments of length $90\Delta x = 90/8192$ at the two ends. Although the error around the two ends is smaller than that shown in Fig.3, the error of this figure becomes slight worse than that of Fig.3 in the interior points remote from two ends. The error response shown in Fig.5 drops 94 points at the left end and 127 points at the right end is better than that shown in Fig.3 and 4, respectively. Now the end values are $y_{94} = 0.03708$ and $y_{8065} = -0.005104$ which is closer to zero value than that of Fig.3 and Fig.4, respectively. If the dropping points is properly chosen so that $y_{256} = 1.5495\times10^{-4}$ and $y_{6808} = -1.4119\times10^{-5}$, the error response is shown in Fig.6 which is smaller than that of Fig.5 but is still worse than that of Fig.2.

If the second sharp filter is employed, its error distribution is shown in Fig.7 which has not much

different from that of Fig.2. Again, error propagation range increases as the iteration number increases (and hence error level decreases). The error responses of those cases of dropping data around the two ends are all similar to that shown in Figs.2 and 7 (except that the accurate range is shrunk) so that they are not shown here.

The above discussions show that the first sharp filter can be an effective filter with small error only if the high frequency part has an almost zero value around the two ends. Otherwise, its performance is not good enough. On the other hand, the second sharp filter is not good enough around the two ends. It can achieve a small error result if the data length is long enough. Therefore, it is concluded that: it is recommended to employ the second sharp filter employing the iterative Gaussian smoothing.

The raw data shown as the thin line in Fig.8 is the u-velocity data measured at the near wake region of a low speed turbulent flow over a bluff body [13]. The measured point is at a distance of $0.5D$ from the base of the bluff body, where D is the width of the bluff body. The FFT algorithm is shown in Fig.9a (where the high frequency part is obtained by employing the iterative Gaussian smoothing with parameter $\sigma = 3, m = 126$ which is corresponding to $\lambda \approx 2.3145$ seconds). By consider $\lambda_c = 1/3$ second and $\overline{\lambda} / \lambda_c = 3$, the iterative Gaussian smoothing with the parameter of $\sigma = 0.2239$, $m = 17$ gives the smooth part shown as heavy solid line in Fig.8. With the cut-off frequency of 3Hz, the second sharp filter let the resulting high frequency part to have a spectrum shown in Fig.9b. Finally, the new spectrogram generator gives the amplitude and real parts shown in Fig.l0, respectively. From these spectrogram, the mode-mode interaction can be precisely extracted.

4. Conclusions

Two simple and fast sharp filters are compared. The numerical tests show that the sharp filter employing the iterative Gaussian filter can generate high accurate smooth part than that of the other sharp filter using the linear trend removal.

5. Acknowledgment

This work is supported by the National Science Council of Taiwan under the grant number NSC-94-2212-E006-084.

7. References

1. Y, N, Jeng, and Y. C. Cheng, “A Simple Strategy to Evaluate the Frequency Spectrum of a Time Series Data with Non-Uniform Intervals,” Transactions of the Aeronautical and Astronautical Society of the Republic of China, vol.36, no.3, pp.207-214, 2004 .
2. Bendat, J. S, and Piersol, A. G., “Random Data Analysis and Measurement Procedures,” 3rd ed., John Wiley & Sons, New York, 2000, Chapters 10 & 11, pp.349-456.
3. Y. N. Jeng and Y. C. Cheng, “The New Spectrogram Evaluated by Enhanced Continuous Wavelet and Short Time Fourier Transforms via Windowing Spectrums,” *Proc. 18th IPPR conference on Computer Vision, Graphics and Image Processing (CVGIP2005)*, Taipei R. O. C, Aug. 2005, pp.378-383.
4. Y. N. Jeng, C.T. Chen, and Y. C. Cheng, “A New and Effective Tool to Look into Details of a Turbulent Data String,” *Proc. 12th National Computational Fluid Dyna-mics Conference*, Kaohsiung Taiwan, paper no. CFD12-2501, Aug. 2005.
5. Y. N. Jeng, C. T. Chen, and Y. C. Cheng, “Studies of Some Detailed Phenomena of a Low Speed Turbulent Flow over a Bluff Body,” *Proc. 2005 AASRC/CCAS Joint Conf.*, Kaohsiung, Taiwan, Dec. 2005, paper no. H-47.
6. Y. N. Jeng, C. T. Chen, and Y. C. Cheng, “Some Detailed Information of a Low Speed Turbulent Flow over a Bluff Body Evaluated by New Time-Frequency Analysis,” *AIAA* paper no.2006-3340, San Francisco June, 2006.
7. Y. N. Jeng, “Time-Frequency Plot of a Low Speed Turbulent Flow via a New Time Frequency Transformation,” Proc. 16th Combustion Conf., paper no.9001, April, 2006, Taiwan.
8. Y. N. Jeng, C. T. Chen, and Y. C. Cheng, “A Time-Series Data Analyzing System Using a New Time–Frequency Transform,” Proceeding of the int. conf. on innovative comput. inform. & control, Bejing, China, paper no.icicic-2006-0190, Aug. 2006.
9. Y. N. Jeng, Huang, P. G., and Chen, H., “Wave De-com position in Physical Space Using Iterative Moving Least Squares Methods,” Proceedings of 11-th National Computational Fluid Dynamics Conference, Tai-Tung, paper no. CFD11-0107, Aug. 2004.
10. Y. N. Jeng[1], P. G. Huang[2], and H. Chen, “Filtering and Decomposition of Waveform in Physical Space Using Iterative Moving Least Squares Methods,” AIAA paper no.2005-1303, Reno Jan. 2005.
11. Y. N. Jeng and Y. C. Cheng, “Approximate Sharp High/Low-Passed Filters,” Proceedings of the 13th National Computational Fluid Dynamics Conference, Taipei County, paper no. CFD11-0804, Aug. 2006.
12. H. T. Huynh, “Accurate Monotone Cubic Inter-polation,” SIAM J. Number. Anal. vol.30, no.1, pp57-100, Feb.1993.
13. Wang, C. T., “Investigation of Low-Frequency Variations Embedded in Vortex Shedding Process,” *Ph.D dissertation*, Department of Aeronautics and Astronautics, National Cheng-Kung University, June 2000.

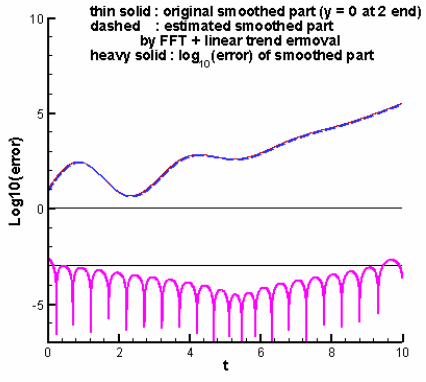

Fig.1 The original and estimated smooth parts (top) and error of the estimation (bottom, in $\log_{10}$ scale), the sinusoidal part has a zero value at the two ends, estimated by the first sharp filter.

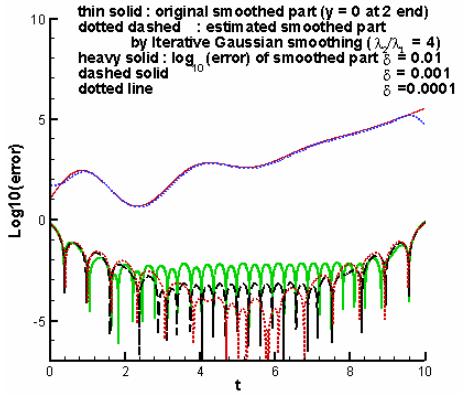

Fig.2 The original and estimated smooth parts (top) and error of the estimation (bottom, in $\log_{10}$ scale), the sinusoidal part has a zero value at the two ends, estimated by the second sharp filter.

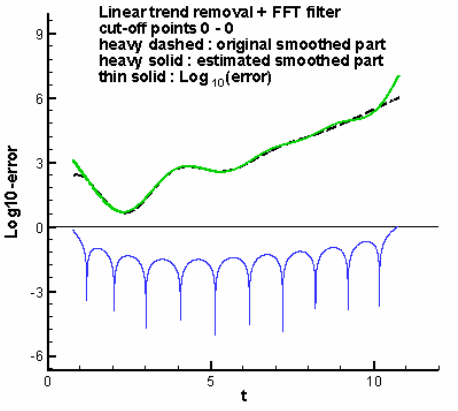

Fig.3 The original and estimated smooth parts (top) and error of the estimation (bottom, in $\log_{10}$ scale), the sinusoidal part does not have a zero value at the two ends, estimated by the first sharp filter.

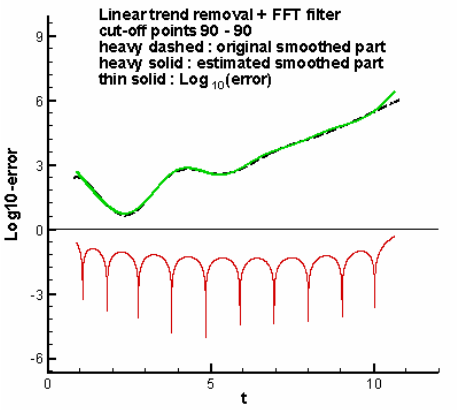

Fig.4 The original and estimated smooth parts (top) and error of the estimation (bottom, in $\log_{10}$ scale), discarding 90 points around the two ends but the sinusoidal part does not have a zero value at the two ends, estimated by the first sharp filter.

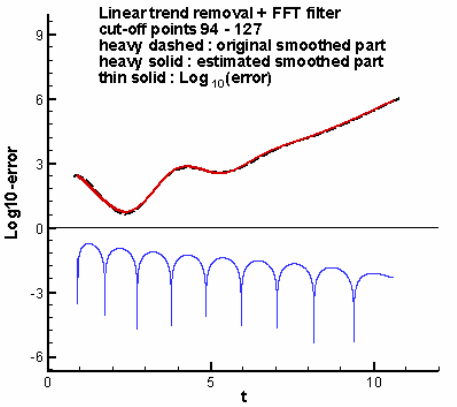

Fig.5 The original and estimated smooth parts (top) and error of the estimation (bottom, in $\log_{10}$ scale), discarding 94 points at the left end and 127 points at the right end, estimated by the first sharp filter.

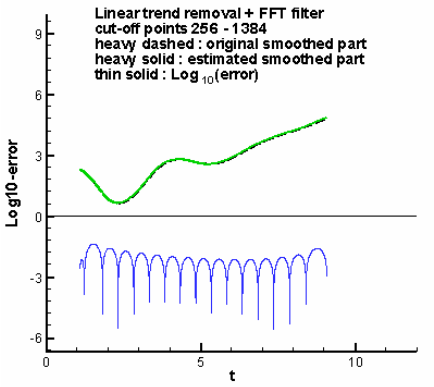

Fig.6 The original and estimated smooth parts (top) and error of the estimation (bottom, in $\log_{10}$ scale), dropping 256 points at the left end and 1384 points at the right end, estimated by the first sharp filter.

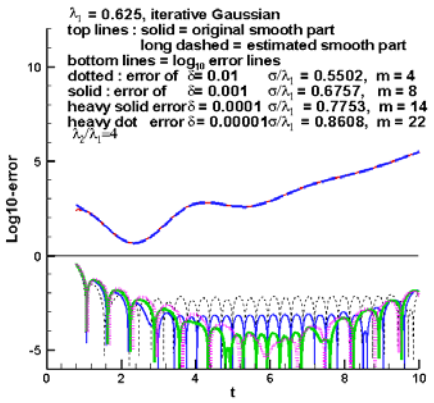

Fig.7 The original and estimated smooth parts (top) and error of the estimation (bottom, in $\log_{10}$ scale), the sinusoidal part has a non-zero value at the two ends, estimated by the second sharp filter.

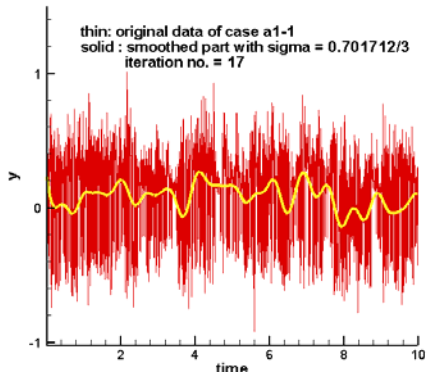

Fig.8 Original and smooth part data (with $\sigma = 0.7017$, $m = 17$).

(a)

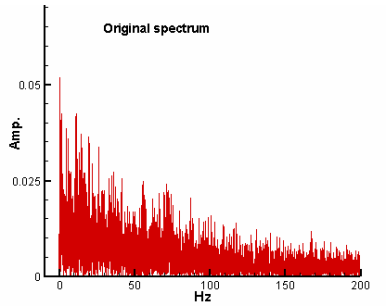

(b)

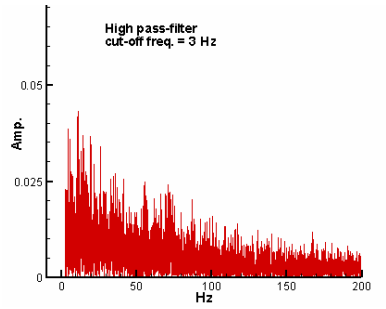

Fig.9 (a) the original spectrum (top); and (b) and spectrum of high-pass filtered data (bottom) with cut-off freq. = 3 Hz.

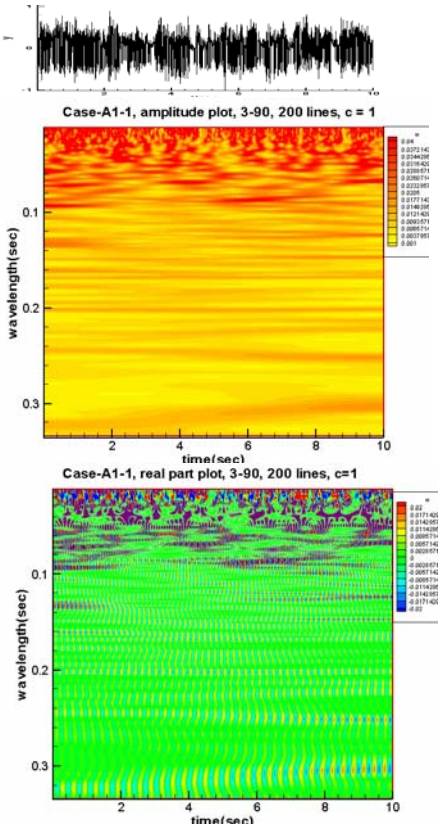

Fig.10 The amplitude and real part plots of the high frequency part.

兩個尖銳的擴散型濾波器之比較

鄭育能[1] 鄭又齊[2]
[1]國立成功大學航空太空學系教授
[2]國立台灣大學電機學系大學畢業生
國科會計畫編號：NSC-94-2212-E-084

摘要

本文比較兩個簡易及快速的擴散型濾波器產生的平滑部份之精確度。第一種方法使用線性移除法配合快速傅式級數轉換法濾出非週期性資料和低頻部份，第二種方法使用疊代式高斯平滑法配合快速傅式級數轉換法移除非週期性和低頻部份。其後兩種方法都在得到頻譜後，直接對頻譜取單為階梯窗口以得到尖銳的高低通濾波結果，或以矩形窗口以得到尖銳的帶通頻譜。數值測試結果顯示第二種使用疊代式高斯平滑法的尖銳濾波器較能釋應一般數據，在其內部點得到高精確的結果。

關鍵字： 尖銳型高低通濾波，快速傅式級數轉換，數位訊號